

Finite Element Analysis of Oil-Lubricated Elliptical Journal Bearings

Marco T. C. Faria

Abstract—Fixed-geometry hydrodynamic journal bearings are one of the best supporting systems for several applications of rotating machinery. Cylindrical journal bearings present excellent load-carrying capacity and low manufacturing costs, but they are subjected to the oil-film instability at high speeds. An attempt of overcoming this instability problem has been the development of non-circular journal bearings. This work deals with an analysis of oil-lubricated elliptical journal bearings using the finite element method. Steady-state and dynamic performance characteristics of elliptical bearings are rendered by zeroth- and first-order lubrication equations obtained through a linearized perturbation method applied on the classical Reynolds equation. Four-node isoparametric rectangular finite elements are employed to model the bearing thin film flow. Curves of elliptical bearing load capacity and dynamic force coefficients are rendered at several operating conditions. The results presented in this work demonstrate the influence of the bearing ellipticity on its performance at different loading conditions.

Keywords—Elliptical journal bearings, non-circular journal bearings, hydrodynamic bearings, finite element method.

I. INTRODUCTION

BEARINGS are mechanical components that must perform three basic tasks: supporting loads (dynamically and statically), providing stiffness and damping to the rotating system, and controlling the journal position [1]. The hydrodynamic pressure associated with the lubricant film flow within the bearing lands provides the capacity of supporting the rotating shaft loads at high speeds. Weight reduction and power increase have been the main design goals in the development of modern industrial rotating machines. The development of faster and more flexible rotating shafts requires more efficient computer procedures that can help engineers to predict the machine behavior and to foresee vibration problems in industrial applications [2].

The analysis of the hydrodynamic journal bearings in the performance of industrial rotating machinery is a fundamental step in the design of more efficient supporting systems. Curves of cylindrical journal bearing steady-state characteristics can be found in the vast technical literature of mechanical design [3]-[5]. However, cylindrical journal bearings are susceptible to hydrodynamic instability at high speeds [6]. The quest for non-cylindrical profiles of journal bearings that can render more adequate supporting systems is

still a challenge for the development of safer, faster and more efficient industrial rotating machinery [7].

This work deals with a performance analysis of hydrodynamic elliptical journal bearings using a special finite element procedure devised to evaluate their steady-state and dynamic behavior. This finite element procedure is derived from a linear perturbation method applied on the classical Reynolds equation, which permits to obtain the zeroth- and first-order lubrication equations [8] for elliptical journal bearings. The Galerkin weighted residual method is employed to integrate the discrete lubrication equations within the fluid film domain [9]. Four-node quadrangular isoparametric finite elements are used to model the fluid film. Curves of steady-state and dynamic performance characteristics of elliptical journal bearings are presented to provide some guidance for engineers dealing with the selection and design of supporting systems for industrial rotating machines.

II. ELLIPTICAL JOURNAL BEARING PARAMETERS

Fig. 1 depicts a schematic view of an elliptical journal bearing. The journal eccentricity is represented by e . The external load on the bearing is given by W . The bearing length and diameter are described, respectively, by L and D ($D=2.R$). The inertial frame axes (X, Y, Z) are fixed to the bearing center, while the rotating frame axes (x, y, z) are attached to the journal ($x=R.\theta$). The journal rotating speed is described by Ω and the bearing attitude angle is represented by ϕ .

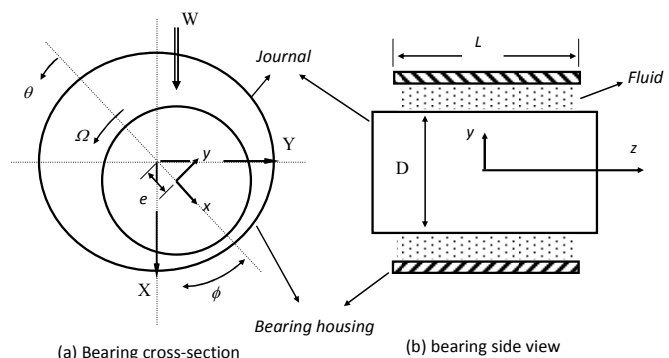


Fig. 1 Schematic drawing of an elliptical journal bearing

The classical Reynolds equation for isoviscous, incompressible film fluid flow [10] can be written in the following form:

$$\frac{1}{R^2} \frac{\partial}{\partial \theta} \left(\frac{\rho h^3}{12\mu} \frac{\partial p}{\partial \theta} \right) + \frac{\partial}{\partial z} \left(\frac{\rho h^3}{12\mu} \frac{\partial p}{\partial z} \right) = \frac{1}{2} \frac{U}{R} \frac{\partial(\rho h)}{\partial \theta} + \frac{\partial(\rho h)}{\partial t} \quad (1)$$

Marco Tulio C. Faria, Ph.D., is Associate Professor of the Department of Mechanical Engineering at Universidade Federal de Minas Gerais (UFMG), Av. Antonio Carlos, 6627, Belo Horizonte, MG, 31270-901, Brazil (phone: 55-31-34094925; fax: 55-31-34094823; e-mail: mtfaria@demec.ufmg.br).

R describes the journal radius, p the hydrodynamic pressure, h the fluid film thickness, U the journal surface tangential speed, ($U=\Omega.R$), ρ the lubricant mass density and μ the fluid film viscosity. The thin fluid film flow domain is given by $0 \leq \theta \leq 2\pi$ and $-L/2 \leq z \leq L/2$. The bearing hydrodynamic pressure is subjected to the periodical boundary condition along the circumferential direction, $p(\theta, z, t) = p(\theta + 2\pi, z, t)$, and the bearing sides are at ambient pressure p_a , that is $p(\theta, L/2, t) = p(\theta, -L/2, t) = p_a$. The Sommerfeld condition is employed in the computation of the fluid film pressure [10]. The fluid film thickness “ h ” can be expressed as:

$$h = c + e_x(t)\cos(\theta) + e_y(t)\sin(\theta) + c.MP\|\sin\theta\| \quad (2)$$

The vertical and horizontal components of the journal eccentricity are given, respectively, by e_x and e_y . The journal eccentricity ratio can be computed by $\varepsilon=e/c$, in which c represents the bearing radial clearance. The bearing preload is described by MP [7]. The value of MP can be considered as a measure of the bearing non-cylindricity and is computed by:

$$MP = (c_{max} - c_{min})/c \quad (3)$$

where c_{max} represents the largest value of the bearing radial clearance and c_{min} is its minimum value. $MP=0$ implies that the bearing has a cylindrical profile.

III. LUBRICATION EQUATIONS

In order to estimate the bearing load capacity and dynamic force coefficients, the zeroth and first-order lubrication equations for elliptical journal bearings must be derived from a linearized perturbation method [8] applied on the Reynolds equation. A journal equilibrium position (e_{x_0}, e_{y_0}) is perturbed by small amplitude motions ($\Delta e_x, \Delta e_y$) at a excitation frequency ω [7]. Thus the film thickness can be rewritten as

$$h = h_0 + (\Delta e_x h_x + \Delta e_y h_y)e^{i\omega t} = h_0 + \Delta e_\sigma h_\sigma e^{i\omega t}; \sigma = x, y, \quad (4)$$

where h_0 represents the steady-state or zeroth-order fluid film thickness, $h_x = \cos(\theta)$, $h_y = \sin(\theta)$, and $i = \sqrt{-1}$. It is assumed that small perturbations on the fluid film thickness will cause small variations on the hydrodynamic pressure field. The perturbed hydrodynamic pressure field can be expressed by

$$p(\theta, t) = p_0(\theta, t) + (\Delta e_x p_x + \Delta e_y p_y)e^{i\omega t} = p_0 + \Delta e_\sigma p_\sigma e^{i\omega t} \quad (5)$$

The steady-state or zeroth-order pressure field is described by p_0 and the perturbed or first-order pressure field is represented by p_x and p_y . Inserting (4) and (5) into (1) renders the zeroth-order lubrication equation (6) and the first-order lubrication equation (7).

$$\frac{1}{R^2} \frac{\partial}{\partial \theta} \left(\frac{\rho h_0^3}{12\mu} \frac{\partial p_0}{\partial \theta} \right) + \frac{\partial}{\partial z} \left(\frac{\rho h_0^3}{12\mu} \frac{\partial p_0}{\partial z} \right) = \frac{1}{2} \frac{U}{R} \frac{\partial(\rho h_0)}{\partial \theta} \quad (6)$$

$$\frac{1}{R^2} \frac{\partial}{\partial \theta} \left(\frac{3\rho h_0^2 h_\sigma}{12\mu} \frac{\partial p_\sigma}{\partial \theta} + \frac{\rho h_0^3}{12\mu} \frac{\partial p_\sigma}{\partial \theta} \right) + \frac{\partial}{\partial z} \left(\frac{3\rho h_0^2 h_\sigma}{12\mu} \frac{\partial p_\sigma}{\partial z} + \frac{\rho h_0^3}{12\mu} \frac{\partial p_\sigma}{\partial z} \right) = \frac{1}{2} \frac{U}{R} \left[\frac{\partial(\rho h_\sigma)}{\partial \theta} \right] + i\omega \rho h_\sigma. \quad (7)$$

Bilinear shape functions Ψ_i^e ($i=1,2,3,4$) [9] are employed to represent the discrete zeroth- and first-order pressure fields. The oil-lubricated elliptical journal bearing hydrodynamic pressure can be estimated from (6). The bearing dynamic force coefficients can be estimated from the perturbed pressure fields rendered by (7). The discrete zeroth- and first-order pressure fields within a finite element domain Ω^e are represented by $p_0^e = \Psi_i^e p_{0i}^e$ and $p_\sigma^e = \Psi_i^e p_{\sigma i}^e$, respectively, in which $i=1,2,3,4$ and $\sigma = x, y$.

On the domain Ω^e of a finite element, the Galerkin weighted residual method is used to obtain the elementary zeroth-order lubrication equation. This equation can be expressed by,

$$k_{ji}^e p_{0i}^e = f_j^e + q_j^e; i, j=1,2,3,4, \quad (8)$$

where

$$k_{ji}^e = \iint_{\Omega^e} \left(\frac{\rho h_0^3}{12\mu} \left(\frac{1}{R^2} \frac{\partial \Psi_i^e}{\partial \theta} \frac{\partial \Psi_j^e}{\partial \theta} + \frac{\partial \Psi_i^e}{\partial z} \frac{\partial \Psi_j^e}{\partial z} \right) \right) d\Omega_e,$$

$$f_j^e = - \iint_{\Omega^e} \frac{\Omega \rho h_0}{2} \cdot \frac{\partial \Psi_j^e}{\partial \theta} d\Omega_e \text{ and } q_j^e = \oint_{\Gamma_e} \Psi_j^e \dot{m}_n d\Gamma_e.$$

The finite element boundary is represented by Γ_e and the normal fluid flow through the border is given by \dot{m}_n .

Similarly, the first-order finite element equation, which represents the perturbed form of the Reynolds equation given by (7), can be written as

$$k_{\sigma ji}^e p_{\sigma i}^e = f_{\sigma j}^e + q_{\sigma j}^e, \quad (9)$$

in which

$$k_{\sigma ji}^e = \iint_{\Omega^e} \left(\frac{\rho h_0^3}{12\mu} \left(\frac{1}{R^2} \frac{\partial \Psi_i^e}{\partial \theta} \frac{\partial \Psi_j^e}{\partial \theta} + \frac{\partial \Psi_i^e}{\partial z} \frac{\partial \Psi_j^e}{\partial z} \right) + \left[\frac{-3\rho h_0^2 h_\sigma}{12\mu} \left(\frac{1}{R^2} \frac{\partial p_0}{\partial \theta} \frac{\partial \Psi_j^e}{\partial \theta} + \frac{\partial p_0}{\partial z} \frac{\partial \Psi_j^e}{\partial z} \right) + \frac{\Omega \rho h_\sigma}{2} \frac{\partial \Psi_j^e}{\partial \theta} - i\omega \cdot \rho \cdot h_\sigma \cdot \Psi_j^e \right] \right) d\Omega_e$$

and

$$q_{\sigma j}^e = \oint_{\Gamma_e} \Psi_j^e \dot{m}_{\sigma n}^e d\Gamma_e.$$

The first-order normal fluid flow through the border Γ_e of a finite element is denoted by $\dot{m}_{\sigma n}^e$.

The global zeroth-order finite element equation, defined over the entire thin fluid film domain Ω , is obtained by superposing the equations provided by (8). The solution of the zeroth-order lubrication equation leads to the steady-state hydrodynamic pressure field, which can be integrated over the fluid domain to render the bearing load capacity and other static performance characteristics, such as the friction torque and the side flow rate. The fluid film reaction forces can be estimated by the following expression, in which the ambient pressure is given by p_a .

$$F_{\sigma_o} = \int_0^L \int_0^{2\pi} (p_o - p_a) h_{\sigma} R d\theta dz; \sigma = x, y. \quad (10)$$

The computation of the perturbed or first-order pressure field is performed by a system of complex finite element equations obtained from (9). The numerical integration of the first-order pressure field renders an estimate for the fluid film complex impedances $\{Z_{\sigma\beta}\}_{\beta, \sigma=x, y}$. The linearized stiffness coefficients, $\{\bar{K}_{\sigma\beta}\}_{\beta, \sigma=x, y}$, and damping coefficients, $\{\bar{C}_{\sigma\beta}\}_{\beta, \sigma=x, y}$, associated with the fluid film hydrodynamic action, assuming a shaft perfectly aligned, can be computed as follows.

$$Z_{\sigma\beta} = \bar{K}_{\sigma\beta} + i\omega \bar{C}_{\sigma\beta} = - \int_0^L \int_0^{2\pi} p_{\beta} h_{\sigma} R d\theta dz; \beta, \sigma = x, y \quad (11)$$

Or

$$\begin{bmatrix} \bar{K}_{xx} & \bar{K}_{xy} \\ \bar{K}_{yx} & \bar{K}_{yy} \end{bmatrix} + i\omega \begin{bmatrix} \bar{C}_{xx} & \bar{C}_{xy} \\ \bar{C}_{yx} & \bar{C}_{yy} \end{bmatrix} = - \int_0^L \int_0^{2\pi} \begin{bmatrix} p_x h_x & p_y h_x \\ p_x h_y & p_y h_y \end{bmatrix} R d\theta dz \quad (12)$$

The synchronous dynamic force coefficients are computed at $\omega = \Omega$.

IV. NUMERICAL RESULTS

The presentation of the numerical results rendered in this work is divided into three parts, for convenience. Firstly, an example of elliptical journal bearing (JB) is selected to perform the mesh sensitivity analysis of the implemented finite element procedure. Secondly, a case of oil-lubricated elliptical journal bearing presented in [11] is analyzed to validate the finite element procedure (FEM) implemented to estimate the bearing load capacity. Finally, some performance characteristics of elliptical journal bearings are estimated.

A. Mesh Sensitivity Analysis

Table I shows the data of the example of elliptical journal bearing selected to perform the mesh sensitivity analysis of the finite element procedure implemented in this work. The values of load capacity (W), direct stiffness coefficient (K_{xx}), and direct damping coefficient (C_{xx}) are estimated for different mesh sizes. The predictions are presented in Table II for eight finite element meshes. The relative deviation between the

values of bearing load and dynamic coefficients computed for a mesh with 810 finite elements and the values computed for a mesh with 2,945 finite elements is smaller than 0.2%. From this analysis, it can be stated that meshes with less than 1,000 finite elements are able to render satisfactory results for the bearing characteristics analyzed.

TABLE I
ELLIPTICAL BEARING DATA FOR MESH SENSITIVITY ANALYSIS

$c = 75.0 \times 10^{-6}$ m	$MP = 0.30$	$D = 0.100$ m
$\rho = 892.0$ kg/m ³	$L/D = 0.75$	$L = 0.075$ m
$\mu = 8.4 \times 10^{-3}$ Pa.s	$\omega = 2000$ rpm	$U = 10.47$ m/s

TABLE II
BEARING LOAD CAPACITY AND DIRECT STIFFNESS AND DAMPING COEFFICIENTS FOR DIFFERENT MESH SIZES

Circumferential Nodes	Axial Nodes	Mesh Size (Number of elements)	W (N)	K_{xx} (MN/m)	C_{xx} (kN.s/m)
39	10	340	1106.0	2.418	2.423
51	13	600	1112.0	2.421	2.437
59	15	810	1114.0	2.422	2.441
71	18	1190	1116.0	2.423	2.445
79	20	1480	1116.5	2.423	2.447
90	23	1960	1117.0	2.423	2.448
98	25	2330	1117.0	2.423	2.449
110	28	2945	1117.0	2.423	2.449

B. Validation

The validation of the finite element procedure (FEM) is performed by comparing the predictions of elliptical journal bearing load capacity with results available in the technical literature [11]. Dimensionless values of load capacity of an elliptical journal bearing are estimated for slenderness ratio (L/D) equals to 1.0. Fig. 2 depicts the curves rendered by the FEM, marked with circles, and by [11], marked with squares. The solution presented in [11] is based on a finite difference procedure. The finite element mesh used in this validation employs 1190 elements (70 circumferential and 17 axial elements). It can be noticed that the values of load capacity agree very well until the journal eccentricity ratio of 0.5. From this value of eccentricity ratio, the comparative values of bearing load present a relative difference smaller than 10%. These results indicate that the procedure implemented in this work can render reliable results for the steady-state analysis of elliptical journal bearings.

C. Performance Analysis of Elliptical JB

Some predictions rendered for elliptical journal bearings are presented in this section. Two very important parameters for elliptical journal bearings are the preload (MP) and the slenderness ratio (L/D). The analysis performed in this work is an attempt of depicting the influence of these parameters on the behavior of elliptical bearings. The performance characteristics selected for the bearing steady-state analysis are the bearing load capacity and friction torque and for the dynamic analysis are the stiffness and damping coefficients. The bearing friction torque is crucial to estimate the power loss caused by the thin film fluid viscous effects. In the vast technical literature of bearing design there are few data about

the performance of elliptical journal bearings [7]. The baseline parameters of elliptical journal bearing are shown in Table III. The finite element mesh for the bearing analysis employs 2,000 isoparametric finite elements.

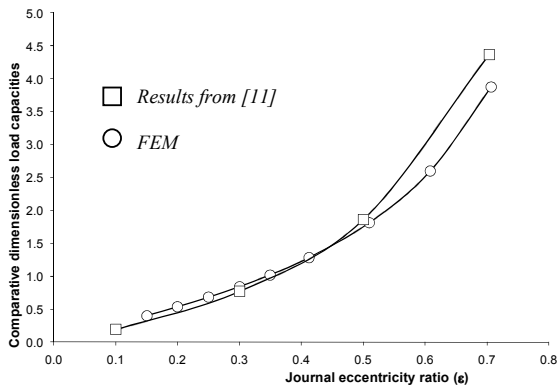


Fig. 2 Comparative curves of dimensionless load capacity versus the journal eccentricity ratio for an elliptical journal bearing with slenderness ratio (L/D) of 1.0

TABLE III

BASLINE PARAMETERS FOR THE ELLIPTICAL JOURNAL BEARING ANALYSIS

$c = 75.0 \times 10^{-6} \text{ m}$	$MP = 0.1; 0.3; 0.5; \text{ and } 0.7$	$D = 0.100 \text{ m}$
$\rho = 892.0 \text{ kg/m}^3$	$L/D = 0.25; 0.5; 1.0; \text{ and } 2.0$	$L = 0.025 \text{ m}; 0.05 \text{ m}; 0.1 \text{ m}; \text{ and } 0.2 \text{ m}$
$\mu = 8.4 \times 10^{-3} \text{ Pa.s}$	$\omega = 2000 \text{ rpm}$	$U = 10.47 \text{ m/s}$

Firstly, the influence of the bearing preload on its steady-state performance is studied for elliptical journal bearings with typical industrial slenderness ratio ($L/D=1$). Fig. 3 depicts the curves of the Sommerfeld number (S_o) in function of the journal eccentricity ratio (ϵ) for different values of preload (MP). The Sommerfeld number is a dimensionless parameter used to characterize journal bearings, which combines some bearing operating and geometric parameters, and can be expressed as $S_o = \frac{R^2}{c^2} \cdot \mu \cdot \frac{N}{P}$. The journal rotating speed is represented by N (given in Hz) and the specific load is described by P ($P = W / (L/D)$). Fig. 3 shows that an increase in the bearing preload causes an increase in the Sommerfeld number. For a bearing operating at constant speed, the value of S_o could be increased by decreasing the journal eccentricity or by using a more viscous lubricant. These results demonstrate that a preload increase (that is, an increase in the bearing non-cylindricity) tends to reduce the journal bearing load capacity. For similar geometric parameters (same values of L , D and c_{min}) and similar operating conditions (N and μ), the cylindrical journal bearings are capable of supporting higher loads than the elliptical journal bearings are.

The preload $MP=0.5$ is considered the optimum value for elliptical journal bearings based on the largest capability of attenuating the journal dynamic response [12]. Fig. 4 depicts the curves of the Sommerfeld number versus the journal eccentricity ratio for elliptical bearings with $MP=0.5$ at different values of slenderness ratio (L/D). As expected the

curves of Fig. 4 only show that short elliptical journal bearings have smaller load capacity than long bearings do.

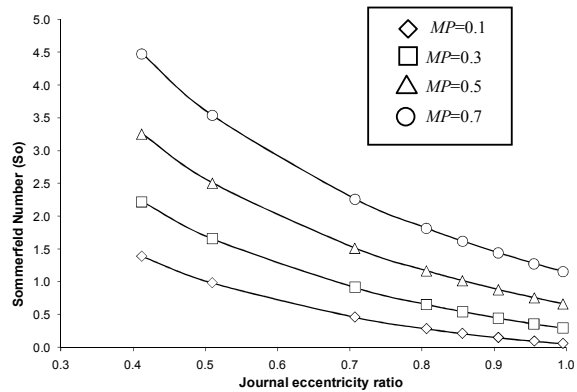


Fig. 3 Curves of the Sommerfeld number versus the journal eccentricity ratio at different values of bearing preload for $L/D = 1.0$

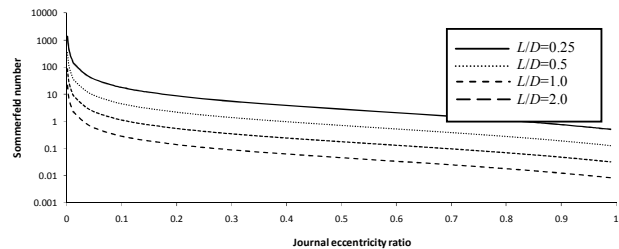


Fig. 4 Curves of the Sommerfeld number versus the journal eccentricity ratio for elliptical journal bearings with $MP=0.5$ at different slenderness ratios

The bearing friction torque can be estimated by using [4]:

$$T = 2\pi \cdot R^2 \cdot L \cdot \tau \quad (13)$$

The fluid film shear stresses are described by τ . The curves of the friction torque for elliptical bearings with $MP=0.5$ at different values of slenderness ratio are shown in Fig. 5. As expected long journal bearings offer more viscous resistance to the journal motion than short bearings do. Very short journal bearings ($L/D=0.25$) are not capable of generating friction torque for high loads (low values of the Sommerfeld number). The larger is the journal bearing slenderness ratio the larger is the bearing capability of dissipating energy.

The curves of the bearing friction coefficient in function of the Sommerfeld number can provide a form to estimate the fluid film viscous power loss. Fig. 6 shows the curves of the dimensionless friction coefficient ($\frac{R}{c} \cdot f$) versus the

Sommerfeld number for elliptical bearings with $MP=0.5$ at different values of slenderness ratio. For shafts under light loads (high values of Sommerfeld number); the slenderness ratio practically does not influence the dimensionless friction coefficient. The bearing friction coefficient can be estimated by $f = \frac{T}{W \cdot R}$.

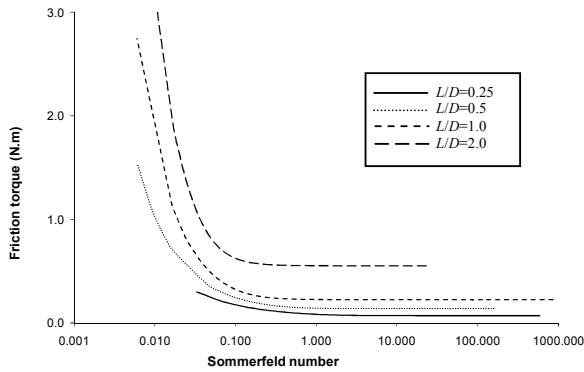


Fig. 5 Curves of the friction torque for elliptical journal bearings with $MP=0.5$ at different values of slenderness ratio

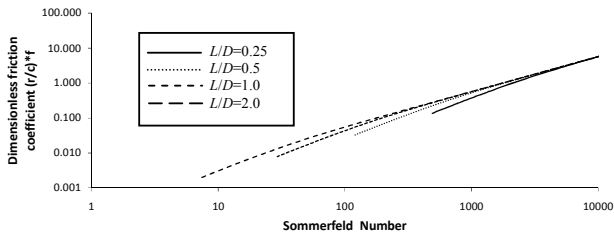


Fig. 6 Curves of the dimensionless friction coefficient for elliptical journal bearings with $MP=0.5$ at different values of slenderness ratio

The determination of the bearing stiffness and damping coefficients is very important for the dynamic analysis of rotating shafts supported on fluid film bearings [13]. Eight linearized force coefficients can be predicted for elliptical journal bearings at several operating conditions. The dimensionless bearing coefficients to be presented are computed in the following way:

$$K_{ij} = \frac{c \cdot \bar{K}_{ij}}{W} \quad \text{and} \quad C_{ij} = \frac{c \cdot \bar{C}_{ij} \cdot \omega}{W}, \quad (i,j=X,Y), \quad (14)$$

where \bar{K}_{ij} and \bar{C}_{ij} represent the stiffness and damping coefficients, respectively, rendered by the finite element procedure, and K_{ij} and C_{ij} represent their dimensionless values.

For elliptical journal bearings with $MP=0.5$ and $L/D=1$, Fig. 7 depicts the curves of the dimensionless stiffness coefficients (K_{XX} , K_{YY} , K_{XY} and K_{YX}) in function of the Sommerfeld number. Low values of the Sommerfeld number are associated with high values of the bearing reaction forces. The variation of the dimensionless damping coefficients (C_{XX} , C_{YY} , C_{XY} and C_{YX}) with respect to the Sommerfeld number is shown in Fig. 8. The stability analysis of rotating shafts supported by fluid film bearings depends on the predictions of the bearing dynamic force coefficients [14]. The adequate selection of the bearing coefficients can reduce the transmitted dynamic forces by the bearings to the non-rotating parts of the rotating machinery. This reduction is important to attenuate the vibration problems caused by the transmitting forces, prolonging the life of the mechanical components and

reducing the fluid film hydrodynamic action. The dynamic coefficients tend to reach their maximum values at low values of the Sommerfeld number. Low Sommerfeld numbers mean high bearing loads, which represent high values of the journal eccentricity. The higher is the bearing load the larger are the dynamic force coefficients. On the other hand, bearings operating with low loads, at almost centered position, present low values of force coefficients.

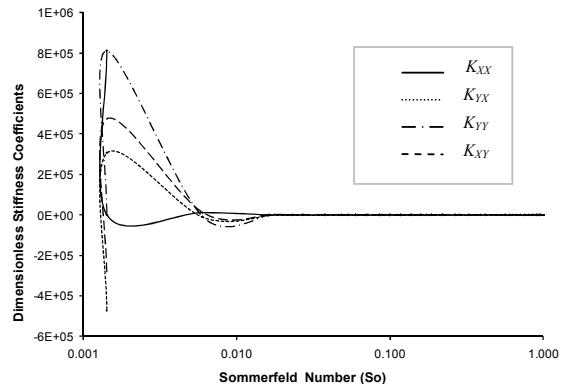


Fig. 7 Curves of dimensionless stiffness coefficients versus the Sommerfeld number for elliptical journal bearings with $MP=0.5$ and $L/D=1.0$

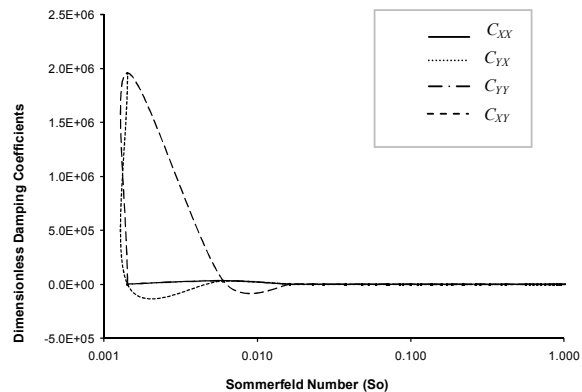


Fig. 8 Curves of dimensionless damping coefficients versus the Sommerfeld number for elliptical journal bearings with $MP=0.5$ and $L/D=1.0$

A relevant analysis of elliptical journal bearings consists in estimating the values of the direct damping coefficients (C_{XX} and C_{YY}) and cross-coupled stiffness coefficients (K_{XY} and K_{YX}) at several operating conditions. The ratio of the direct damping coefficient to the cross-coupled stiffness coefficient permits to evaluate the level of effective damping [14] provided by the fluid film bearing to the rotating shaft. The effective damping coefficient (C_{ef}) is an important parameter for the bearing stability analysis and can be written as:

$$C_{ef} = \frac{2 \Omega C_{XX}}{K_{XY}} \quad (15)$$

The curves of the dimensionless direct damping coefficient (C_{XX}) and cross-coupled stiffness coefficient (K_{XY}) are shown in Figs. 9 and 10, respectively, in function of the Sommerfeld number. It can be noticed that the patterns of the curves of C_{XX} and K_{XY} are similar. Fig. 9 shows that at very low Sommerfeld numbers the values of cross-coupled stiffness are large and not much influenced by L/D . The analysis also shows that, for elliptical journal bearings, the values of K_{XY} are small for any values of L/D and S_o .

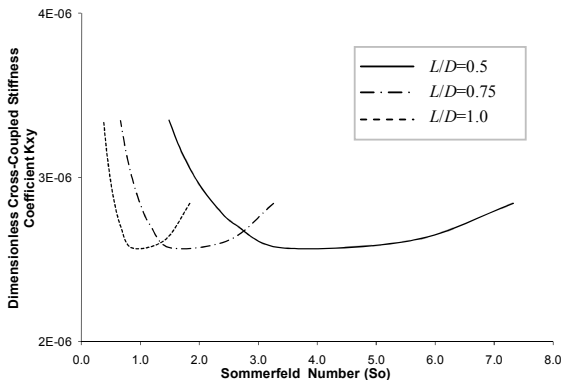


Fig. 9 Curves of the dimensionless cross-coupled stiffness coefficient (K_{XY}) versus the Sommerfeld number for elliptical journal bearings with $MP=0.5$ at different slenderness ratios

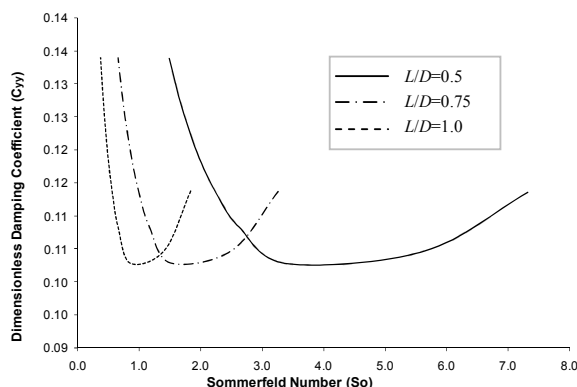


Fig. 10 Curves of the dimensionless direct damping coefficient (C_{XX}) versus the Sommerfeld number for elliptical journal bearings with $MP=0.5$ at different slenderness ratios

The direct damping coefficients (C_{XX} and C_{YY}) have great influence on the bearing capability of attenuating the dynamic response of rotating shafts supported by fluid film bearings. From Fig. 10 it can be observed that longer elliptical journal bearings ($L/D \rightarrow 1$) are capable of providing viscous resistance to the journal rotation at very low Sommerfeld numbers (high loads). On the other hand, shorter bearings ($L/D=0.5$) are not capable of providing enough damping for low values of the Sommerfeld number.

V. CONCLUSIONS

The application of the finite element method in the development of efficient computer procedures for the analysis

of hydrodynamic elliptical journal bearings is the core of this work. The solution of the Reynolds equation requires approximate solution methods for the prediction of the performance characteristics of the vast majority of industrial fluid film journal bearings ($0.5 \leq L/D \leq 1$). The numerical results rendered in this work are useful to understand some aspects about the steady-state and dynamic behavior of elliptical journal bearings with different preloads and slenderness ratios at several operating conditions. These results bring some insights into the steady-state and dynamic performance characteristics of different elliptical bearings. It is noteworthy to say that this work is an attempt of bringing some technical data about the behavior fluid film elliptical bearings, which are scarce in the technical literature.

ACKNOWLEDGMENT

The author expresses his gratitude to FAPEMIG and UFMG for the financial support.

REFERENCES

- [1] B. Sternlicht and P. Lewis, "Vibration problems with high speed turbomachinery," *ASME Journal of Engineering for Industry*, 1968, pp. 174-186.
- [2] K. Knöös, "Journal bearings for industrial turbosets," *Brown Boveri Review*, vol. 67, 1980, pp.300-308.
- [3] R.C. Juvinall and K.M. Marshek, *Fundamentals of Machine Component Design*. New York: John Wiley & Sons, 5th Ed., 2012.
- [4] R.G. Budynas and J.K. Nisbett, *Shigley's Mechanical Engineering Design*. New York: McGraw-Hill, 9th Ed., 2011.
- [5] R. Norton, *Machine Design – An Integrated Approach*. New York: Prentice-Hall, 2nd Ed., 2000.
- [6] P.E. Allaire and R.D. Flack, "Design of journal bearings for rotating machinery," in *Proc 10th Turbomachinery Symposium*, Houston, 1981, pp. 25-45.
- [7] F.A.G. Correia, "Determinação das características de desempenho de mancais radiais elípticos utilizando o método de elementos finitos", M.Sc. Thesis, Graduate Program in Mechanical Engineering, Universidade Federal de Minas Gerais, Belo Horizonte, Brazil, 2007.
- [8] P. Klit and J.W. Lund, "Calculation of the dynamic coefficients of a journal bearing, using a variational approach," *ASME Journal of Tribology*, vol. 108, 1986, pp.421-425.
- [9] K.J. Bathe, *Finite element procedures in engineering analysis*. New York: Prentice-Hall, 1982.
- [10] B.J. Hamrock, *Fundamentals of Fluid Film Lubrication*. New York: McGraw-Hill, 1994.
- [11] A. Singh and B.K. Gupta, "Stability limits of elliptical journal bearing supporting flexible rotors," *Wear*, vol. 77, 1982, pp. 159-170.
- [12] W.M. Miranda and M.T.C. Faria, "Lateral vibration analysis of flexible shafts supported on elliptical journal bearings", *Tribology Letters*, vol. 48, 2012, pp.217-227.
- [13] D. Childs, 1993, *Turbomachinery rotordynamics*. New York: John Wiley & Sons, 1993.
- [14] J.M. Vance, *Rotordynamics of turbomachinery*. New York: John Wiley & Sons, 1988.

Marco Tulio C. Faria has a B.Sc. degree in Mechanical Engineering from the University of Brasília-Brazil (1986), a M.Sc. degree in Mechanical Engineering from Federal University of Santa Catarina-Brazil (1990), and a Ph.D. degree in Mechanical Engineering from Texas A&M University (1999). Currently he holds a position of Associate Professor in the Department of Mechanical Engineering at the Federal University of Minas Gerais. His research interests are lubrication theory, physical modeling of hydraulic turbines and rotor dynamics. E-mail: mtfaria@demec.ufmg.br.